Supporting information

Exploring the mechanisms of the reductase activity of neuroglobin by site-directed mutagenesis of the heme distal pocket

Jesús Tejero[1,*], Courtney Sparacino-Watkins[1], Venkata Ragireddy[1], Sheila Frizzell[1] and Mark T. Gladwin[1,2]

From the [1]Vascular Medicine Institute, University of Pittsburgh, Pittsburgh, PA 15213; [2]Pulmonary, Allergy and Critical Care Medicine, University of Pittsburgh, Pittsburgh, PA 15213.

*Address correspondence to: Jesús Tejero, Vascular Medicine Institute, University of Pittsburgh. E1244 BST, 200 Lothrop Street, Pittsburgh PA 15261; Tel. 412-648-3181; Fax: 412-648-5980; E-mail: jet68@pitt.edu

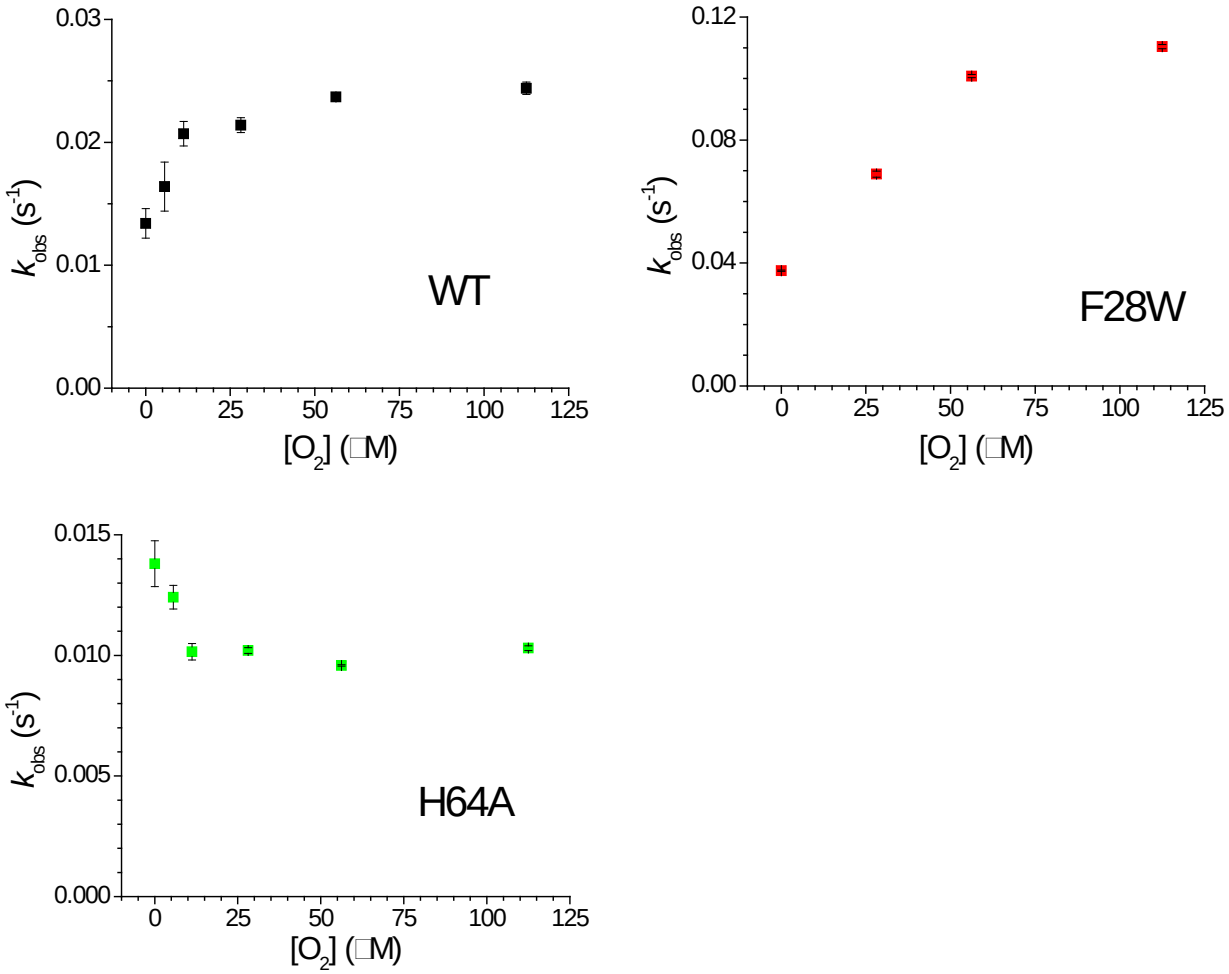

Supplemental Figure 1. Autoxidation rates of wild-type neuroglobin and the mutants F28W and H64A as a function of the oxygen concentration. Deoxy-Ngb (Fe^{II}) samples were mixed with variable concentrations of oxygen; after the fast initial formation of the oxy-Ngb (Fe^{II}-O_2) species the decay to the met-Ngb (Fe^{III}) form was monitored. The points indicate the observed rates and standards deviations. Top left panel, wild-type neuroglobin; top right panel, F28W neuroglobin; bottom left panel, H64A neuroglobin.

Supplemental Methods for Supplemental Figure 1 - Autoxidation rates at different oxygen concentrations were monitored by stopped-flow spectroscopy using an Applied Photophysics SX20 instrument (Applied Photophysics Ltd., Leatherhead, Surrey, UK) enclosed in an anaerobic glove box (Coy Laboratory Products, Grass Lake, MI). The autoxidation was monitored by mixing deoxy-Ngb(Fe^{II}) samples of Ngb with a range of oxygen concentrations. The concentrations were achieved mixing different ratios of air-saturated buffer with anaerobic buffer. An oxygen concentration of value of 225 µM was used for air-saturated buffer at 37°C [1]. Deoxy-Ngb (Fe^{II}) was prepared by reduction of met-Ngb(Fe^{III}) with sodium dithionite. Excess dithionite was removed by gel filtration with a Sephadex G25-column (PD10, GE Healthcare) equilibrated with anaerobic sodium phosphate buffer (100 mM, pH 7.4). The mixing of Ngb and oxygen leads to the fast formation of the oxy-Ngb (Fe^{II}-O_2) species and a subsequent slow decay of this species to form met-Ngb(Fe^{III}). We monitored the decay of the soret peak of the oxy-Ngb species for 200 seconds (Wild-type, H64A) or 50 s (F28W) and the traces were fit to a single exponential decay equation using the ProData SX software (Applied Photophysics). Reactions rates were followed at 37 °C.

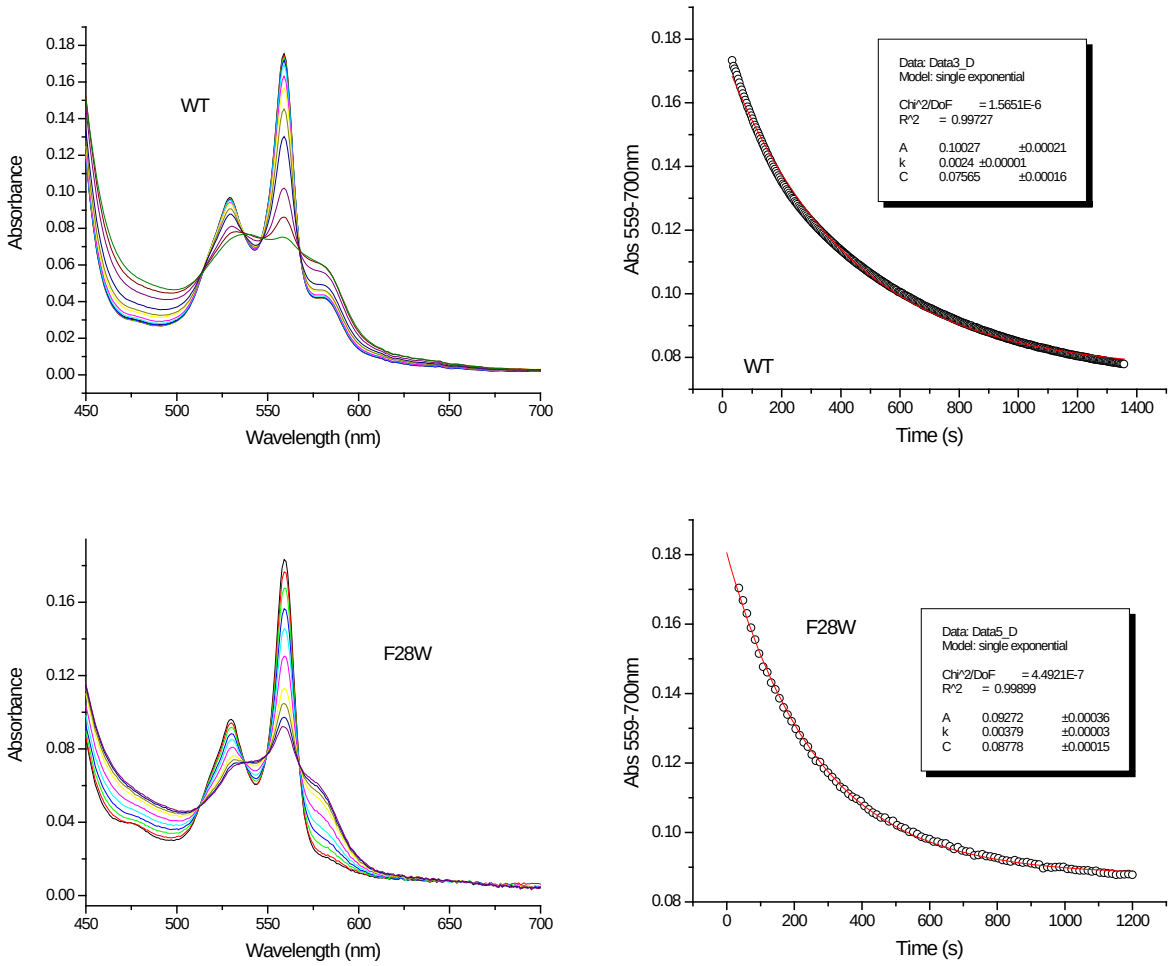

Supplemental Figure 2. Nitrite reduction by wild-type neuroglobin and the mutant F28W. Left hand panels show the absorbance changes during the reaction of nitrite with the deoxy-neuroglobin (Fe^{II}) in the presence of 2.5 mM sodium dithionite. Right hand panels show the absorbance decay at 559 nm during the reaction; the red line indicates the fit to a single exponential decay equation. The concentrations of nitrite were 5 mM in both experiments. The reaction was carried out at 37 °C in 100 mM sodium phosphate buffer, pH 7.4.

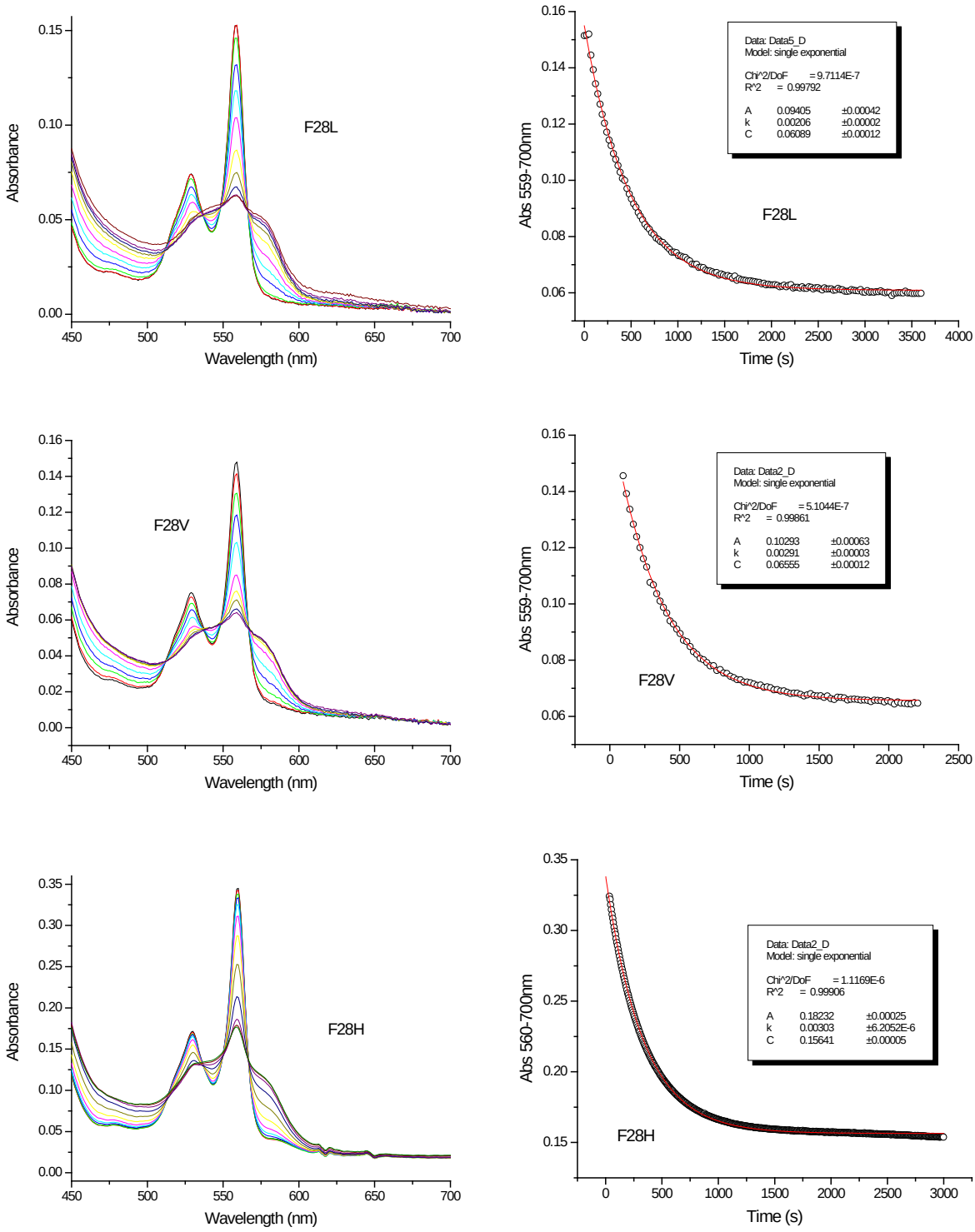

Supplemental Figure 3. Nitrite reduction by the neuroglobin mutants F28L, F28V and F28H. Left hand panels show the absorbance changes during the reaction of nitrite with the deoxy-neuroglobin (Fe^{II}) in the presence of 2.5 mM sodium dithionite. Right hand panels show the absorbance decay at 559 or 560 nm during the reaction; the red line indicates the fit to a single exponential decay equation. The concentrations of nitrite were 1 mM (F28L and F28V) or 10 mM (F28H). The reaction was carried out at 37 °C in 100 mM sodium phosphate buffer, pH 7.4.

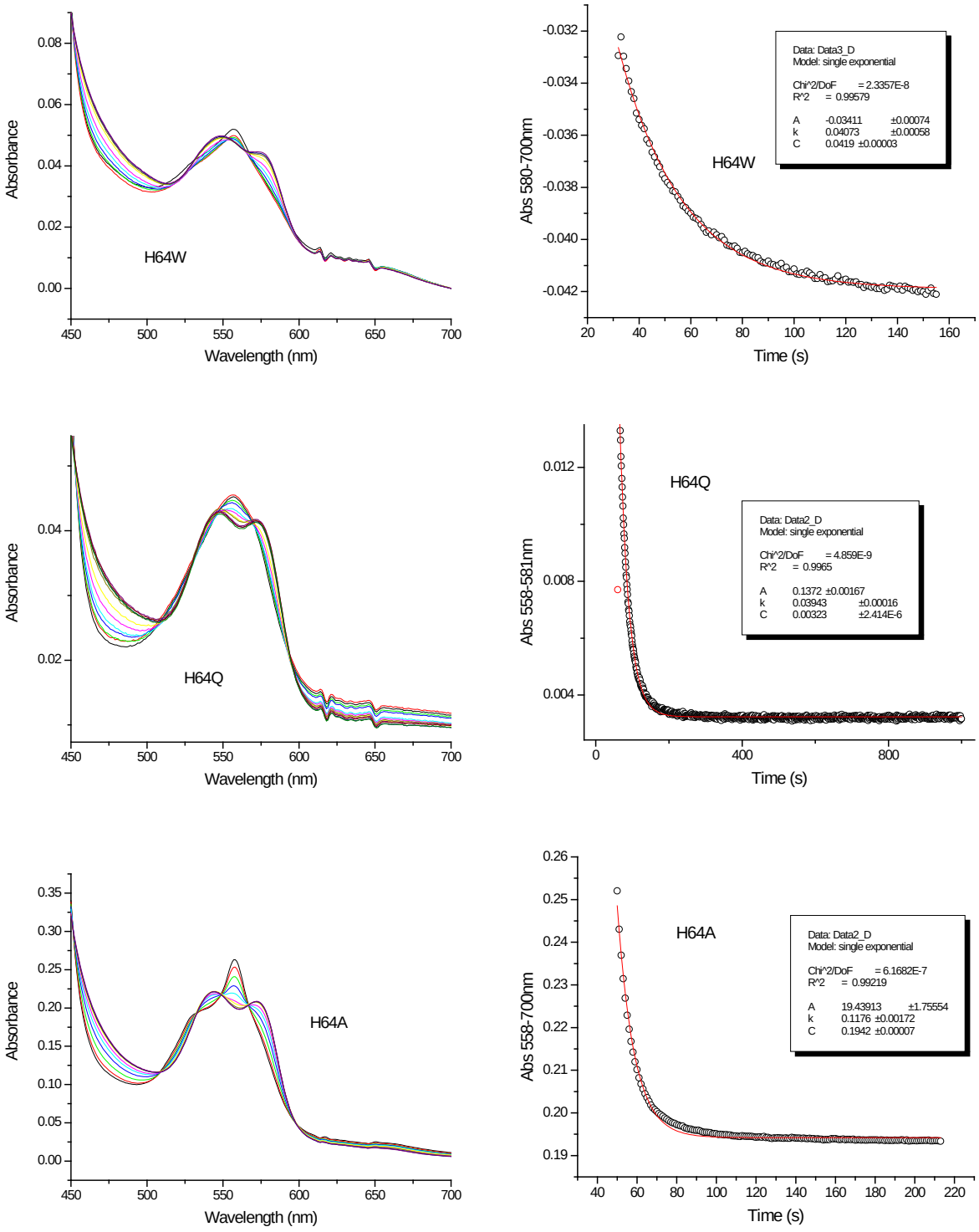

Supplemental Figure 4. Nitrite reduction by the neuroglobin mutants H64W, H64Q, and H64A. Left hand panels show the absorbance changes during the reaction of nitrite with the deoxy-neuroglobin (Fe^{II}) in the presence of 2.5 mM sodium dithionite. Right hand panels show the absorbance decay at 558 or 580 nm during the reaction; the red line indicates the fit to a single exponential decay equation. The concentrations of nitrite were 5 mM (H64W) or 0.1 mM (H64Q and H64A). The reaction was carried out at 37 °C in 100 mM sodium phosphate buffer, pH 7.4.

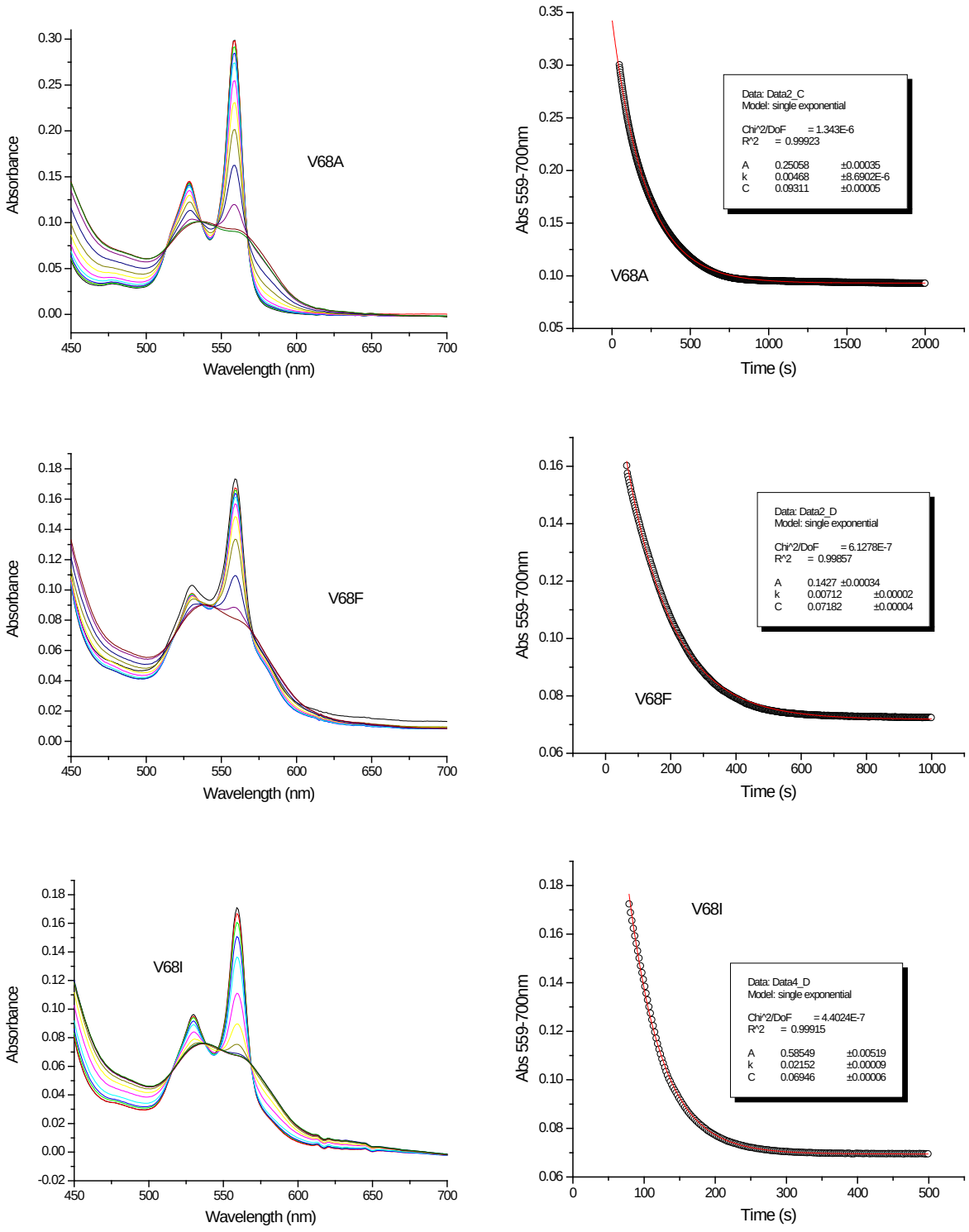

Supplemental Figure 5. Nitrite reduction by the neuroglobin mutants V68A, V68I, and V68F. Left hand panels show the absorbance changes during the reaction of nitrite with the deoxy-neuroglobin (Fe^{II}) in the presence of 2.5 mM sodium dithionite. Right hand panels show the absorbance decay at 559 nm during the reaction; the red line indicates the fit to a single exponential decay equation. The concentrations of nitrite were 50 mM (V68A) or 5 mM (V68F and V68I). The reaction was carried out at 37 °C in 100 mM sodium phosphate buffer, pH 7.4.

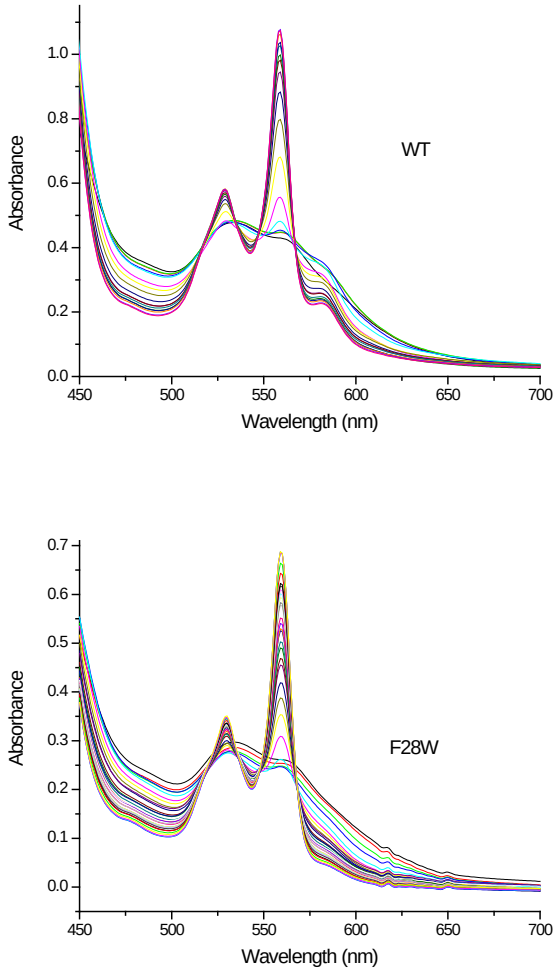

Supplemental Figure 6. Redox titration of wild-type neuroglobin and the mutant F28W. The panels show the spectra obtained after successive additions of sodium dithionite to an initial sample of fully oxidized protein. The spectrum shifts from the oxidized species (maximum around 535 nm) to the deoxy species with maxima around 530 and 560 nm. The titrations were carried out at 25°C in 100 mM sodium phosphate buffer, pH 7.0.

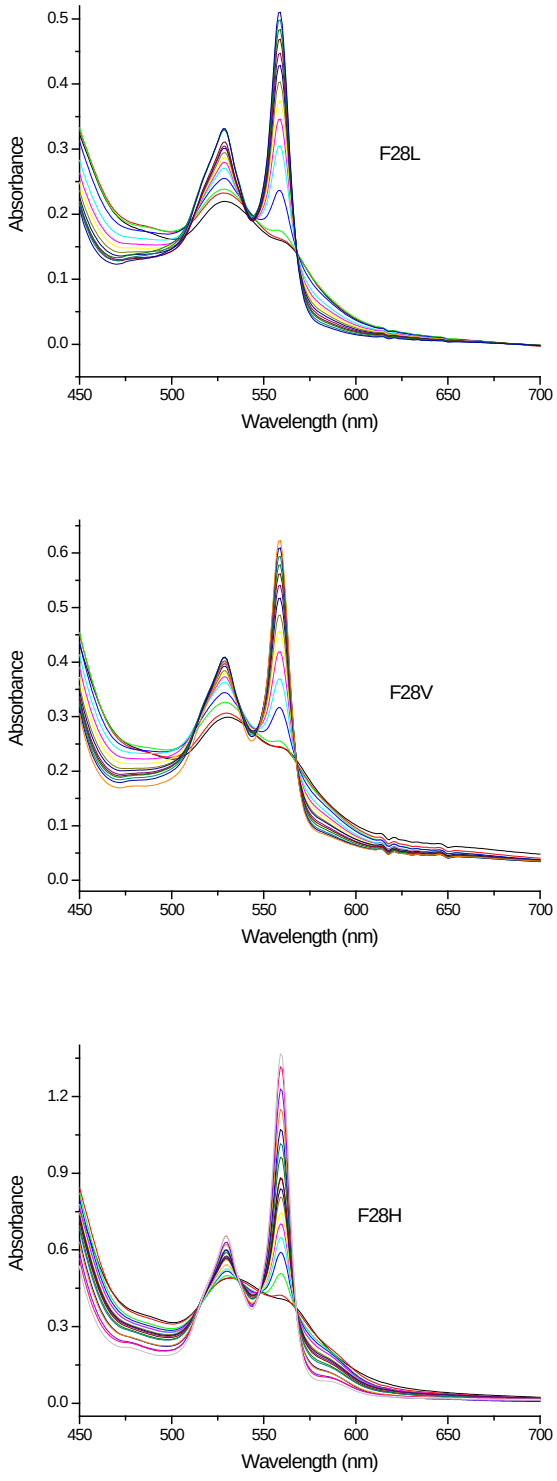

Supplemental Figure 7. Redox titration of the neuroglobin mutants F28L, F28V and F28H. The panels show the spectra obtained after successive additions of sodium dithionite to an initial sample of fully oxidized protein. The spectrum shifts from the oxidized species (maximum around 535 nm) to the deoxy species with maxima around 530 and 560 nm. The titrations were carried out at 25°C in 100 mM sodium phosphate buffer, pH 7.0.

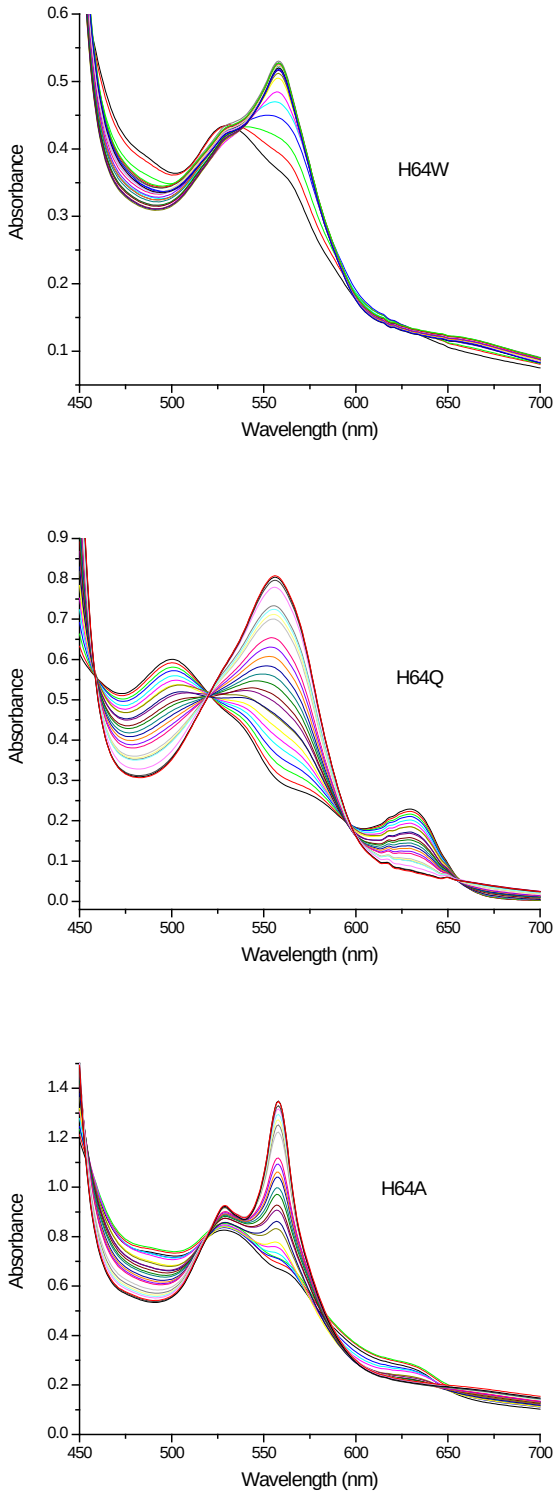

Supplemental Figure 8. Redox titration of the neuroglobin mutants H64W, H64Q and H64A. The panels show the spectra obtained after successive additions of sodium dithionite to an initial sample of fully oxidized protein. The spectrum shifts from the oxidized species (maximum around 535 nm for H64W and H64A; 500nm and 630nm for H64Q)) to the deoxy species with maxima around 560 nm (H64W and H64Q) or 530 and 560 nm (H64A). The titrations were carried out at 25°C in 100 mM sodium phosphate buffer, pH 7.0.

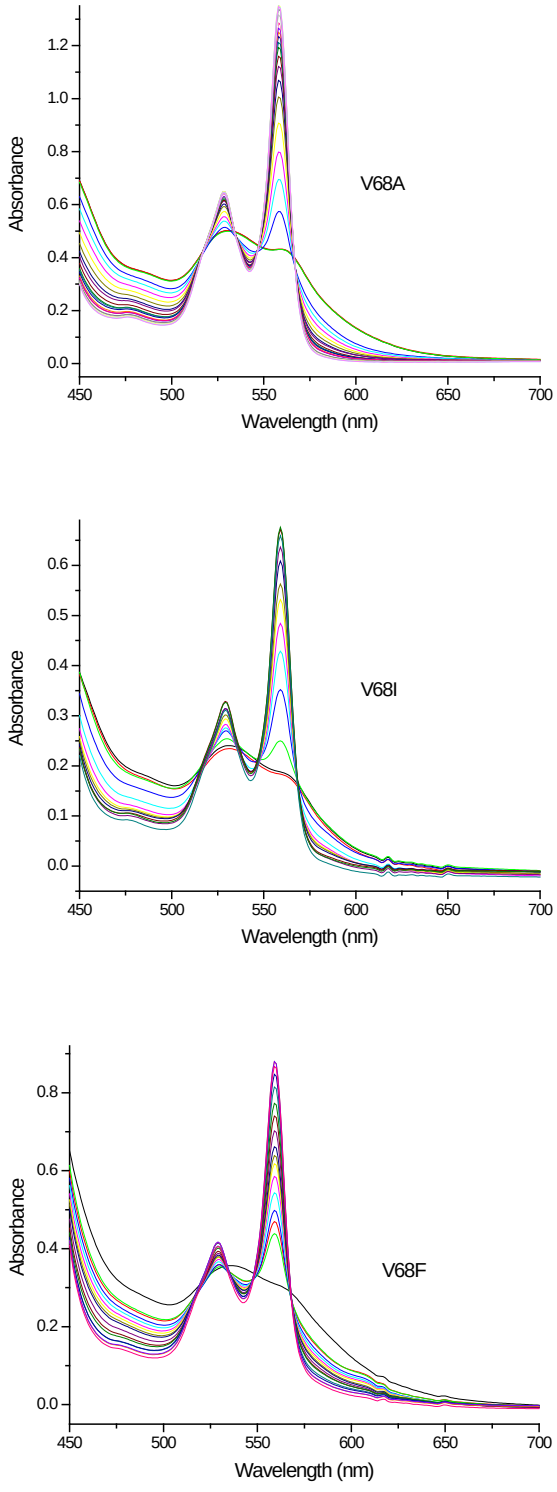

Supplemental Figure 9. Redox titration of the neuroglobin mutants V68A, V68I, V68F. The panels show the spectra obtained after successive additions of sodium dithionite to an initial sample of fully oxidized protein. The spectrum shifts from the oxidized species (maximum around 535 nm) to the deoxy species with maxima around 530 and 560 nm. The titrations were carried out at 25°C in 100 mM sodium phosphate buffer, pH 7.0.

Supplemental Table 1. Nitrite reduction rates, redox potentials and autoxidation rates of myoglobin mutants in the positions B10, E7 and E11.

Mb mutation	k_{autox} [a] (h^{-1})	$K_{Nitrite}$ ($M^{-1}s^{-1}$)	E_m (mV)
Wild-type	0.051	5.6 [b] / 5.5 [c]	59 [d] / 59 [e] / 55 [f]
L29F	0.005	-	-
L29V	0.23	-	-
L29A	0.24	-	-
H64Q	0.21	-	-
H64A	58	1.8 [b]	-
H64L	10	<< 0.2 [b]	84 [g]
H64G	44	-	65 [g]
H64V	33	0.35 [c]	76 [g] / 87 [h]
H64T	54	-	-
H64F	6	-	109 [g]
H64M	-	-	98 [g]
H64Y	-	-	20 [f]
H64I	-	-	95 [h]
V68A	0.26	-	-
V68F	0.069	-	-
V68I	0.75	-	-
V68L	0.10	-	-
V68E	-	-	-137 [d]
V68D	-	-	-132 [d]
V68N	-	-	-24 [d]
V68H	-	-	-110 [i]

[a] Sperm whale myoglobin; values determined at 37 °C in 100 mM sodium phosphate buffer, pH 7.0 [2].
[b] Sperm whale myoglobin; values determined at 25 °C in 100 mM potassium phosphate buffer, pH 7.0 [3].
[c] Horse myoglobin; values determined at 25 °C in 100 mM phosphate buffer, pH 7.41 [4]
[d] Human myoglobin; values determined at 25 °C in phosphate buffer μ =0.1 M , pH 7.0 [5].
[e] Sperm whale myoglobin; values determined at 25 °C in phosphate buffer μ =0.1 M , pH 7.0 [5].
[f] Horse myoglobin; values determined at 25 °C in phosphate buffer μ =0.1 M , pH 7.0 [6].
[g] Sperm whale myoglobin; values determined at 22 °C in 100 mM Na-Hepes buffer, pH 7.0 [7].
[h] Horse myoglobin; values determined at 25 °C in 46mM sodium phosphate buffer, pH 7.0 [8].
[i] Horse myoglobin; values determined at 25 °C in phosphate buffer μ=0.1 M , pH 7.0 [9].

References

1. Battino, R., (Ed.) (1981) *IUPAC Solubility Data Series, Vol.7, Oxygen and Ozone*, Pergamon Press, Oxford, England.
2. Brantley, R. E., Jr., Smerdon, S. J., Wilkinson, A. J., Singleton, E. W., and Olson, J. S. (1993) The mechanism of autooxidation of myoglobin, *J Biol Chem 268*, 6995-7010.
3. Tiso, M., Tejero, J., Basu, S., Azarov, I., Wang, X., Simplaceanu, V., Frizzell, S., Jayaraman, T., Geary, L., Shapiro, C., Ho, C., Shiva, S., Kim-Shapiro, D. B., and Gladwin, M. T. (2011) Human neuroglobin functions as a redox-regulated nitrite reductase, *J Biol Chem 286*, 18277-18289.
4. Yi, J., Heinecke, J., Tan, H., Ford, P. C., and Richter-Addo, G. B. (2009) The distal pocket histidine residue in horse heart myoglobin directs the O-binding mode of nitrite to the heme iron, *J Am Chem Soc 131*, 18119-18128.
5. Varadarajan, R., Zewert, T. E., Gray, H. B., and Boxer, S. G. (1989) Effects of buried ionizable amino acids on the reduction potential of recombinant myoglobin, *Science 243*, 69-72.
6. Tang, H. L., Chance, B., Mauk, A. G., Powers, L. S., Reddy, K. S., and Smith, M. (1994) Spectroscopic, Electrochemical, and Ligand-Binding Properties of the Horse Heart Metmyoglobin His(64)-Tyr Variant, *Bba-Protein Struct M 1206*, 90-96.
7. VanDyke, B. R., Saltman, P., and Armstrong, F. A. (1996) Control of myoglobin electron-transfer rates by the distal (nonbound) histidine residue, *Journal of the American Chemical Society 118*, 3490-3492.
8. Hildebrand, D. P., Ferrer, J. C., Tang, H. L., Smith, M., and Mauk, A. G. (1995) Trans effects on cysteine ligation in the proximal His93Cys variant of horse heart myoglobin, *Biochemistry 34*, 11598-11605.
9. Lloyd, E., Hildebrand, D. P., Tu, K. M., and Mauk, A. G. (1995) Conversion of Myoglobin into a Reversible Electron-Transfer Protein That Maintains Bishistidine Axial Ligation, *Journal of the American Chemical Society 117*, 6434-6438.